Project (Grant) Number:	824135
Project Acronym:	SOLARNET
Project Title:	Integrating High Resolution Solar Physics

Document Details	
Document Title	Release of Basic Computational Tools and high-level analysis tools
Prepared by (Institution's Name):	University of Sheffield (USFD)
Work Package Number & Title	WP5 - Towards a European Solar Data Centre
Deliverable number (if applicable)	D5.12 - Release of Basic Computational Tools and high-level analysis tools
Serial Number of Deliverable:	D54
Document Code: (inserted by project office)	D5.12_Version2.0
File Name: (inserted by project office)	SOLARNET_D5.12_V2.0_Public_20200805
Date Uploaded: (inserted by project office)	August 5th, 2020

AUTHORS/ CONTRIBUTORS LIST

Name	Function	Organization
Viktor Fedun	Task Leader (Scientist)	USFD
Robertus Erdelyi	Task Leader (Scientist)	USFD
Michal Sobotka	Task Contributor (Scientist)	Astronomical Institute of the Czech Academy of Sciences (ASU)
Jana Kašparová	Task Contributor (Scientist)	ASU
Elena Dzifčáková	Task Contributor (Scientist)	ASU
Alena Zemanová	Task Contributor (Scientist)	ASU

APPROVAL CONTROL FROM SUB-WP AND WP LEAD

Control	Name	Organization	Function	Date
Prepared	R. Erdelyi	USFD	Task Leader	July 15th, 2020
Revised	Michal Sobotka	ASU	ASU team leader	July 15th, 2020
Revised	N. Bello González	Leibniz-Institute for Solar Physics (KIS)	WP5 Coordinator	August 4th, 2020
Approved/ Authorized	N. Bello González	KIS	WP5 Coordinator	August 4th, 2020

ADMINISTRATIVE APPROVAL CONTROL FROM PROJECT OFFICE

Control	Name	Organization	Function	Date
Approved	Tirtha Som	KIS	Project Manager	August 4th, 2020
Approved	Rolf Schlichenmaier	KIS	Project Coordinator	August 4th, 2020
Authorized	Markus Roth	KIS	Project Scientist	August 4th, 2020

HISTORY OF DOCUMENT CHANGES

Issue	Date	Change Description
Version 1.0	August 1st, 2020	Initial Issue
Version 2.0	August 4th, 2020	After revision by N. Bello González and M. Roth

Table of Contents

Introduction

On top of fully calibrated, science-ready data disseminated via the SOLARNET Virtual Observatory (VO), one can add value to the data by generating high-level-data tools that allow for determination of physical parameters, visualisation and interoperability, e.g., between datasets of various sources like theoretical models and observations. All of the scientific exploration and data reduction tools developed within the SOLARNET will considerably benefit and have their total development time reduced, if high-quality generic-purpose versatile libraries are available for them to utilise. Within sub-WP5.4, a number of these tools have been developed and are now released to the community.

These tools are described in the following and links to repositories where they can be accessed are provided.

The institutes contributing to this Deliverable D5.12 are USFD and ASU of the SOLARNET Consortium.

1. Core Development Tools (CDT)
Contribution by USFD

CDT aims to extend and improve the existing tools available in SunPy so that they can be utilised by other solar software development packages, whether aiding observations or numerical simulations. This task includes

(1) Improved representation and abstraction of metadata in SunPy to better support ground-based solar observatories such as SST, GREGOR and EST, allowing SunPy to read various types of data in a uniform manner, enabling scientists to write code that runs on both ground- and space-based data sources.

Work has progressed on the NDCube package in collaboration with the DKIST data centre and NASA Goddard to add support to NDCube for loading coordinate information from wider sources of data than just space-based observations in FITS files. Building on work in AstroPy to provide a standard Python API for world coordinate systems, NDCube has been completely rewritten to better support this more abstract representation of world coordinate metadata. This easily supports more complex situations like the SST tabular WCSes and other non-celestial dimensions like Stokes axes, temporal axes and spectral axes. This also provides support for axes where two or more coordinates vary over the axis, such as time and space varying over the rastering axis of a slit spectrograph. See section 6.2 of the SunPy paper for details of NDCube: https://ui.adsabs.harvard.edu/abs/2020ApJ...890...68S/abstract

(2) Extending the NDCube affiliated package to support 3D magnetic field data (e.g. the on-the-fly quick-look like 5.4.3. MONAMI) and integrating it into the *solarbextrapolation* affiliated package, which provides a generic framework for all different types of magnetic field extrapolation codes.

A Python package converting 3D magnetic field output of MONAMI (including potential and non-linear force-free field extrapolation) into NDCube is available at https://github.com/PyDL/MONAMI-to-NDCube

The *solarbextrapolation* project has been archived by SunPy, however, work has been done to better represent this type of data in NDCube. NDCube has developed a new NDCollection class (initial version released in version 1.3.0) that will be expanded to facilitate easy representation of vector data on the same coordinate grid. The *pssfpy* project for full Sun potential field extrapolations plans to make use of this functionality, but this is beyond the scope of CDT.

(3) Improving the representation and visualisation tools in region-of-interest (ROI) objects in the SunPy core package to enable simple and quick on-the-fly analysis.

References

SunPy
https://sunpy.org

The SunPy Community, "The SunPy Project: Open Source Development and Status of the Version 1.0 Core Package", ApJ, 890:68, 2020
https://doi.org/10.3847/1538-4357/ab4f7a

2. Mapping Of Non-potentiAl Magnetic fIeld (MONAMI)
Contribution by USFD

This tool provides a quick look of the magnetic skeleton of the associated field-of-view that can be further analysed and explored (see e.g. Korsos et al. JSWSC 2019, ApJ 2020), even as input for forward modelling. Such skeleton is vital for pointing our large, high-resolution telescopes for pinpointing targets of opportunities (e.g. aiding the goals of WP8, the real-life hunt for flares). MONAMI is fast and provides QL assessment with about a minute-cadence.

Mapping Of Non-potentiAl Magnetic fIeld (MONAMI) can be found in the repository:
https://github.com/komabi/MONAMI-Manual

References

Korsos M.B., Yong, S, Erdelyi, R., "Investigation of pre-flare dynamics using the weighted horizontal magnetic gradient method: From small to major flare classes", JSWSC, 9:A6 (2019)
https://doi.org/10.1051/swsc/2019002

Korsos M.B. et al., "Solar Flare Prediction Using Magnetic Field Diagnostics Above the Photosphere", ApJ, in press, 15pp (2020)

3. Automated Swirl Detection Algorithm v2 (ASDA v2)
Contribution by USFD

Rotational motions are observed on the Sun on a variety of scales, from sub-arcsecond vortex flows to large-scale sunspot rotations, tornadoes, solar jets and coronal mass ejections. The small-scale photospheric vortices are widely hypothesised to form as a natural consequence to granular flows in the quiet Sun and could play a key role in the supply of energy to the upper solar atmosphere, either through the build-up of magnetic energy in twisted field lines in the corona or through the channeling of magnetohydrodynamic (MHD) waves (see e.g. Liu et al. Nat Comm 2019, Astron Astrophys. 2019).

For the above purpose, this task focused on to carry out the development of

o An open-source software tool, using Python and based on ASDA v1 (Liu et al ApJ 2019), for solar atmospheric swirl detection, which is suitable and even more accurate for analysis of data from various ground-based and space-borne instruments.

o   User-friendly interface application of the automated detection to FoV data of high-resolution and high-cadence observation at different layers of the photosphere and chromosphere. Data could be intensity, velocity or magnetic field.

The Automated Swirl Detection Algorithm v2 (ASDA v2) can be found in: https://github.com/PyDL/ASDA

ASDA v2 has been a major improvement compared to v1 in terms of accuracy (new method of detecting edges was implemented) and speed (3 times faster). ASDA is useful for automatic swirl/vortex detection from observational images or computational modelling of the solar atmosphere.

References

Liu J. et al., "Automated Swirl Detection Algorithm (ASDA) and Its Application to Simulation and Observational Data", ApJ, 872:22, 2019
https://doi.org/10.3847/1538-4357/aabd34

Liu J. et al., "ASDA v2", 2020
https://github.com/PyDL/ASDA

Liu J., Mumford S. and Erdelyi, R., "Python converting output of MONAMI into NDCube", 2020
https://github.com/PyDL/MONAMI-to-NDCube

4.   Estimation of the Mass and Energy Supply to Sun's upper Atmosphere and Corona (EMESSUA) & Sheffield Dispersion Diagram Code (SDDC)
Contribution by USFD

Four modules v1.0 as a part of EMESSUA + additionally Sheffield Dispersion Diagram Code (SDDC) are developed, tested and ready to download from the PDG web page:
http://pdg.group.shef.ac.uk/UI.html#Codes

In particular:

1. Wave Mode Analysis Code (WMAC) – dedicated for automatically ranking identified wave modes in the various solar structures (of irregular shape) i.e. sunspots, pores, vortex structures etc. This module is based on implementation of POD and DMD techniques. The code is fully tested for the modes in sunspots. Manual – version 1.0 is ready. Code and manual is uploaded on PDG web page.

2. Code for Vortex Flow Analysis (CVFA) – the module which is based on the Lagrangian Averaged Vorticity Deviation (LAVD) method. Implemented: vortex tubes surface and axis identification. The code is tested for 3D numerical data (MURaM).

3. Tool for Analysis of Oscillatory Modes (TAOM) – the module dedicated to the visualisation of modes in the cross-cuts of the magnetic tube structures of irregular shape.

4. Vortex Detection Code (VDC) – the module dedicated to the identification of vortex motions in the 2D numerical or observational data. Code is fully developed based on implementation of Gamma functions and new algorithm for more accurate tracking of boundary of vortices.

5. Additionally to the core package of EMESSUA, the code Sheffield Dispersion Diagram Code (SDDC) is prepared. This code is s designed to produce the dispersion diagram for MHD wave modes within a solar

application. The code is capable of handling planar or cylindrical geometry and relies on the model being symmetrical about the centre of the waveguide.

5. Solar radiative-hydrodynamics (RHD) codes
Contribution by ASU

High-level analysis tools of FLARIX simulation outputs have been made publicly accessible. IDL tools for user-friendly reading of atmosphere evolution, beam-heating parameters, hydrogen level populations, spectral profiles, and contribution functions are finished. Tools for data related to Ca II and Mg II atoms are being finalised.

Thirteen routines written in the Interactive Data Language (IDL) and an example of a FLARIX model (*flarix_data/* directory) are publicly accessible at http://www.asu.cas.cz/~kasparov/solarnet_idlflarix/. Routines have been tested in IDL version 7.0 at a Linux PC. Examples how to read and display the data are given in the IDL routine *example_flarix.pro*. Other FLARIX simulations can be available upon a request.

5.1. Description

FLARIX is a radiation hydrodynamic code, which can model the time evolution of a 1D atmosphere heated by a specified process, e.g. by electron beams propagating from the injection site in the corona down to the lower atmosphere. The FLARIX code has been developed at the Astronomical Institute of the Czech Academy of Sciences in Ondřejov, Czech Republic, with the primary purpose of flare modelling on (sub-) second timescales.

FLARIX treats the flaring loop from its base deep in the photosphere up to its apex in the corona as a 1D atmosphere, evolving in time and with macroscopic flows (chromospheric condensations and evaporation into coronal parts). The code uses a standard set of 1D hydrodynamic equations. The coupling between the radiation and matter is provided through terms related to net radiation losses and non-LTE ionisation degree. Radiative transfer is treated in detail for atoms and ions important for optically-thick radiative losses in the solar atmosphere, i.e. H, Ca II, and Mg II. Adopted approach takes into account the non-equilibrium ionisation of hydrogen.

The driving mechanism for the flare heating and subsequent dynamical processes (all time dependent) is the injection of accelerated electron beams, which travel from the reconnection site in the corona down to lower layers of the solar atmosphere where they deposit the energy by collisions. The beams are characterized by a few key parameters, namely by energy flux, low-energy cutoff, and spectral index.

Regarding the numerical scheme, FLARIX uses a fixed, but optimized, spatial grid with almost 2000 points (the actual number of points depends on the atmospheric structure). The hydrodynamic equations and non-LTE equations are solved separately, the non-LTE problem is solved implicitly by linearizing the preconditioned kinetic equations and constraint equations. The optically-thick radiative transfer problem is solved using the Accelerated Lambda Iteration (ALI) techniques. The beam energy deposit rate can be computed by the analytic expression or using a hybrid test-particle unit, which allows realistic simulation of the time-dependent electron (proton) beam propagation, scattering, and energy deposit.

More information about FLARIX and examples of simulations can be found in the following papers.

References

Kašparová et al., 2019, ASP Conference Series, Vol. 519, 141
https://ui.adsabs.harvard.edu/abs/2019ASPC..519..141K/abstract

Kašparová et al., 2009, A&A, 499, 923
https://ui.adsabs.harvard.edu/abs/2009A%26A...499..923K/abstract

Varady et al., 2010, IEEE Transactions on Plasma Science, 38, 2249
https://ui.adsabs.harvard.edu/abs/2010ITPS...38.2249V/abstract

6. The KAPPA Package Guide
Contribution by ASU

Analysis of the non-Maxwellian effects in the observed optically thin line spectra presents a new research direction in the spectroscopy of the solar corona and transition region. Non-Maxwellian distributions in the solar corona and transition region can originate as a result of the strong gradient in density or temperature, due to plasma heating by reconnection during the solar flares or micro-flares, due to presence of some types of waves, or due to other physical processes such as turbulence.

The shape of a non-Maxwellian distribution function strongly influences the character of the emitted optically thin spectra. This occurs through the changes in rates, and in stationary conditions to ionization and excitation equilibra. The interpretation of spectra under the assumption of non-Maxwellian distribution usually leads to different diagnosed plasma parameters than those for Maxwellian one, especially for temperature. Therefore, the assumption of Maxwellian distribution of particles can lead to misinterpretation of physical conditions in the observed plasma.

6.1. What is the KAPPA package?

The KAPPA package (kappa.asu.cas.cz) is a software and database allowing us to calculate line intensities and synthetic spectra for electron non-thermal distributions with high energy tail approximated by a κ-distribution. It is based on the CHIANTI software and database for spectral analysis under the assumption of Maxwellian distribution. KAPPA package uses and needs many CHIANTI routines and also its database. Therefore, it cannot be used as a stand-alone software.

6.2. Kappa distributions

In-situ measurements of a distribution function in the solar wind plasma showed the presence of high-energy tail in the distribution. The origin of such distribution, in non-homogenous plasma, is related to the increase of the mean free path of particles with high energy. These particles are then able to penetrate without collisions to regions with different densities and temperatures and thus they produce high-energy tail.

The distributions with high-energy tail can be described by a κ-distribution:

$$f(E)dE = A_\kappa \frac{2}{\pi^{1/2}(k_\mathrm{B}T)^{3/2}} \frac{E^{1/2}dE}{\left(1+\frac{E}{(\kappa-1.5)k_\mathrm{B}T}\right)^{\kappa+1}}, \qquad (1)$$

where E is the particle energy, k_B Boltzmann constant, κ parameter of distribution, and A_κ is the normalization constant, $A_\kappa = \Gamma(\kappa + 1)/\left(\Gamma(\kappa - 1.5)(\kappa - 1.5)^{3/2}\right)$. Temperature T in the κ-distribution has the same relation to the mean energy of particles as Maxwellian distribution:

$$\langle E \rangle = 3 k_B T / 2 \qquad (2)$$

and parameter κ models the shape of the distribution. $\kappa \to 1.5$ is the limit for strongly non-Maxwellian distribution, and for the $\kappa \to \infty$ limit, the κ-distribution approaches Maxwellian. For the constant mean energy but different value of parameter κ, the number of high-energy particles increases when κ decreases, the number of the low energy particles increases too and maximum of distribution moves to lower energies ($E_{max} = k_B T (\kappa - 1.5)/\kappa$), Figure 1. More details about kappa-distributions can be found e.g. in Livadiotis & McComas (2013).
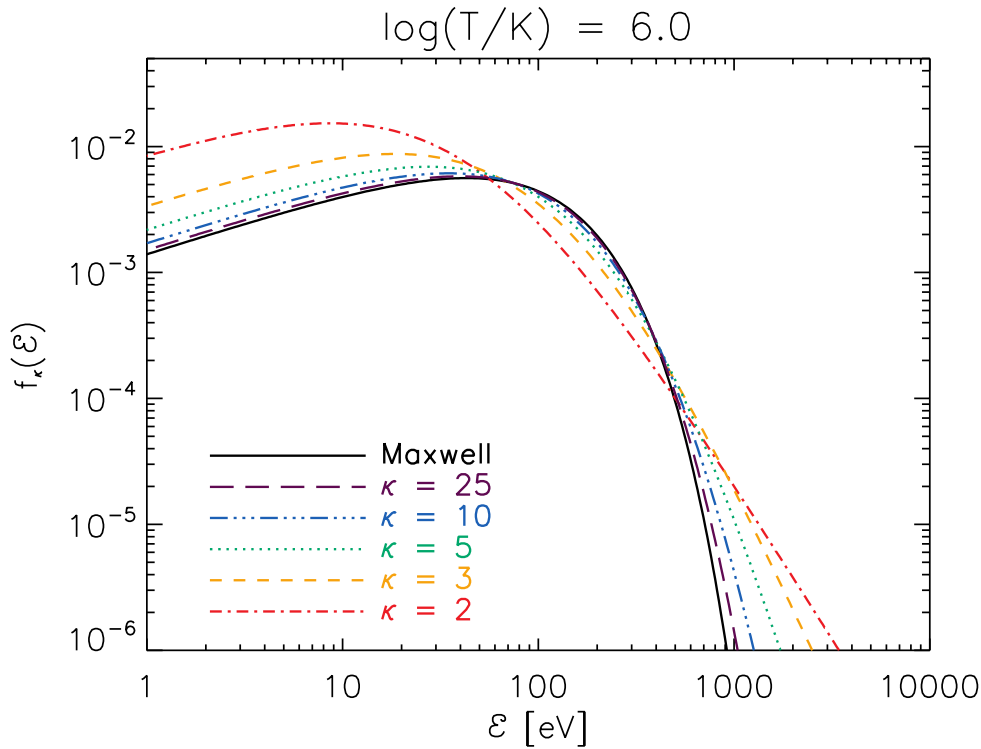
Figure. 1. *Comparison of the Maxwellian distribution with the □-distributions for different κ = 25, 10, 5, 3 and 2, and the same mean energy of particles corresponding to $T = 10^6$ K.*

6.2.1 Ionization equilibrium

In the coronal conditions, the ionization equilibrium is given by equilibrium between total ionizing processes (direct ionization and autoionization) on one hand and, total recombination processes (radiative and dielectronic recombination) on the other hand:

$$n_k C_k^I = n_{k+1} C_{k+1}^R, \qquad (3)$$

where n_k (n_{k0+1}) is density of k-times ($k+1$-times) ionized ions, C_k^I is the total ionization rate of k-times ionized ions and C_{k+1}^R is the total recombination rate of $k+1$-times ionized atoms. The rates of the elementary processes are defined by:

$$C = \langle \sigma v \rangle = \int_0^\infty \sigma \frac{2E^{1/2}}{m} f(E) \, dE, \qquad (4)$$

where σ is collisional cross section, v is the particle velocity, m particle mass, $f(E)$ is the particle distribution function.

The presence of the κ-distribution strongly affects the ionization rates. The effect depends on temperature, ion, and value of κ. Increase of the ionization rate by several orders of magnitude can occur at temperatures several times lower than temperature corresponding to the abundance maximum of given ion for the Maxwellian distribution. This results from the presence of the high-energy tail that increases the number of the high-energy electrons that are able to produce ionizing transitions. The radiative recombination rates are less influenced. An increase of the recombination rate by a factor 2 for κ-distribution with $\kappa = 2$ compared to Maxwellian is typical. Collisional cross sections for this process decrease with electron energy, but the κ-distribution contains more low-energy electrons than the Maxwellian distribution with the same temperature (Figure 1). Therefore, the radiative recombination rates for the κ-distributions are higher. The changes in the dielectronic recombination rates are influenced by the shape of distribution, their peaks are wider and lower for κ-distributions (Dzifčáková and Dudík, 2013, for details).

6.2.2. Excitation equilibrium

For temperatures and electron densities corresponding to the transition region, corona and solar flares, the excitation and de-excitation processes are dominated by electron collisional excitation and radiative de-excitation transitions. The statistical excitation equilibrium in this approximation is described by the equation:

$$n_i\left(\sum_j n_e C_{ij,j\neq i} + A_{ij,j>i}\right) = \sum_j n_j\left(n_e C_{ji,j\neq i} + A_{ji,j>i}\right), \qquad (5)$$

where n_e is the electron density, n_i and n_j are the populations of levels i, and j, C_{ij} and C_{ji} are the electron excitation and de-excitation rates between the levels i and j, and A_{ij}, A_{ji} are Einstein coefficients for the spontaneous radiation. For transitions in optical or near UV region, it is necessarily to include photoexcitation. Its probability is proportional to $B_{ij}\bar{I}_{\nu_{ij}}$, where B_{ij} is Einstein absorption coefficient and $\bar{I}_{\nu_{ij}}$ is the mean intensity of radiation with frequency corresponding to the energy E_{ij} of the transition between the levels i and j.

The electron distribution influences the electron collisional excitation and de-excitation rates (Equation 3). In solar spectroscopy, collision strengths $\Omega_{ij}(E_i) = \Omega_{ji}(E_j)$ instead of the collisional cross sections are usually used:

$$\sigma_{ij} = \frac{\Omega_{ij}}{\omega_i E_i} \pi a_0^2, \qquad (6)$$

where E_i (E_j) is the initial (final) electron energy before (after) the collision, ω_i is statistical weight of level i, and a_0 is the Bohr radius.

The electron excitation and de-excitation rates for κ-distributions can be written using distribution-averaged collisional strengths for excitation, $\Upsilon_{ij}(T, \kappa)$, and de-excitation, $\Upsilon_{ji}(T, \kappa)$ (e.g. Dzifčáková et al., 2015, Dudík et al., 2014):

$$C_{ij} = \frac{2\sqrt{2}a_0^2 I_H}{\sqrt{m_e}\omega_i}\left(\frac{\pi}{k_B T}\right)^{1/2} e^{-\frac{E_{ij}}{k_B T}} \Upsilon_{ij}(T, \kappa) \tag{7}$$

and

$$C_{ji} = \frac{2\sqrt{2}a_0^2 I_H}{\sqrt{m_e}\omega_j}\left(\frac{\pi}{k_B T}\right)^{1/2} \Upsilon_{ji}(T, \kappa) \tag{8}$$

where

$$\Upsilon_{ij} = A_\kappa \frac{E_{ij}}{k_B T} e^{\frac{E_{ij}}{k_B T}} \int_{E_{ij}}^{\infty} \frac{\Omega_{ij}(E_i)}{\left(1 + \frac{E_i}{(\kappa - 1.5)k_B T}\right)^{\kappa+1}} \frac{dE_i}{E_{ij}} \tag{9}$$

and

$$\Upsilon_{ji} = A_\kappa \frac{E_{ij}}{k_B T} \int_0^{\infty} \frac{\Omega_{ji}(E_j)}{\left(1 + \frac{E_j}{(\kappa - 1.5)k_B T}\right)^{\kappa+1}} \frac{dE_j}{E_{ij}} \ . \tag{10}$$

The calculations of excitation rates for the non-Maxwellian distribution is usually problematic (with several exceptions) due to unavailability of the cross sections or collision strengths data. Moreover, these data files are usually huge, having sizes of several tens of GiB. Therefore, only the integral products of the cross sections over the Maxwellian distribution, i.e. the electron excitation rates, are usually published. This is the case in CHIANTI (Dere et al. 1997, Landi et al. 2013, Del Zanna et al. 2015). Consequently, Dzifčáková (2006a), Dzifčáková (2008), and Dzifčáková et al. (2015) developed the unique inversion method which enables to approximate the collision strengths by an analytical function. The method employs the typical limit behaviour of the collision strengths for different types of atomic transitions.

A functional form for the approximation of Ω is assumed

$$\Omega = \sum_{n=0}^{n_{max}} C_n u^{-n} + D\ln(u) \tag{11}$$

where C_n and D are coefficients and $u = E_i / E_{ij}$. The Ω averaged over Maxwellian distribution, $\Upsilon_{ij}(T)$, is

$$\Upsilon_{ij} = \frac{E_{ij}}{k_B T} e^{\frac{E_{ij}}{k_B T}} \int_{E_{ij}}^{\infty} \Omega_{ij}(E_i) e^{-\frac{E_i}{k_B T}} \frac{dE_i}{E_{ij}} \ . \tag{12}$$

After the integration we have

$$\Upsilon_{ij} = C_0 + \left(\sum_{n=1}^{n_{max}} \frac{E_{ij}}{k_B T} C_n E_n\left(\frac{E_{ij}}{k_B T}\right) + D E_1\left(\frac{E_{ij}}{k_B T}\right)\right) e^{\left(\frac{E_{ij}}{k_B T}\right)}. \tag{13}$$

where E_n is an n-the order exponential integral. The high-energy limit of Ω and corresponding behaviour of $\Upsilon_{ij}(T)$ provide conditions for the coefficients C_n and D. For electric dipole transitions we have

$$D = \frac{4\omega_i f_{ij}}{E_{ij}}, \quad \Upsilon_{ij}(\to \infty) = \sum_{n=0}^{n_{max}} C_n = \Omega(u=1), \tag{14}$$

for non-electric dipole, non-exchange transitions

$$C_0 = C_1 = D = 0, \quad \Upsilon_{ij}(\to 0) = \frac{E_{ij}}{k_B T}\int_1^\infty \Omega\, du, \quad \Upsilon_{ij}(\to \infty) = \sum_{n=2}^{n_{max}} C_n = \Omega(u=1). \tag{16}$$

The low-temperature and high-temperature limits of $\Upsilon_{ij}(T)$ can be found in the CHIANTI database. The coefficients C_n and D were evaluated from the Maxwellian collisional strengths in CHIANTI by the least square method. The approximations up to $n_{max} = 7$ were used to achieve the higher precision.

The method was tested for the first time by Dzifčáková and Mason (2008) and subsequently more extensively by Dzifčáková et al. (2015). The comparison of the excitation rates calculated using the approximations with direct calculations of collision strengths showed that in most cases the precision is better than a few percent. Bigger differences appear with decreasing κ, and for $\kappa = 2$, the extreme differences do not exceed 10% which is comparable with typical precision of atomic data themselves.

The presence of the κ-distributions in plasma changes the excitation rates. The character of changes depends on the type of the atomic transition, its excitation energy, temperature and parameter κ (Dzifčáková and Kulinová, 2003, Dzifčáková, 2006, Dzifčáková et al., 2015). Typically, the excitation rate increases for low temperatures. This increase can be several orders of magnitude for $\kappa = 2$ in comparison with the Maxwellian case. However, for temperatures $k_B T \geq E_{ij}$ (Dzifčáková, 2006a), the excitation rates for the κ-distributions are lower than for Maxwellian distribution. The differences increase with decreasing κ.

For known excitation rates, the equations of the statistical equilibrium (Equation 5) can be solved for non-Maxwellian distributions and the intensity of the spectral lines can be calculated in the usual way as an integral along line of sight l:

$$I_{ij} = \frac{hc}{4\pi\lambda_{ij}}A_{j\to i}\int n_{j,X}^k\, dl = \frac{hc}{4\pi\lambda_{ij}}A_{j\to i}\int \frac{n_{j,X}^k}{n_X^k}\frac{n_X^k}{n_X}\frac{n_X}{n_H}\frac{n_H}{n_e}n_e\, dl, \tag{17}$$

where $n_{j,X}^k$ is the density of k-times ionized ions of element X in level j, n_X^k is the density of all k-times ionized ions of element X, n_X is the density of all ions of element X, and n_H is the Hydrogen density. The distribution function affects the line intensity through the ratio of the relative population of level j given by the excitation equilibrium as well as the ratio n_X^k/n_X (abundance of k-times ionized ions of element X) given by the ionization equilibrium for the equilibrium plasma.

6.2.3. Satellite lines

The rate of dielectronic excitation from level i to level j for a distribution function $f(E)$ can be written (Seely at al., 1987)

$$C^{diel} = \left(\frac{2}{m_e \Delta E_{ji}}\right)^{1/2}\frac{h^3 \omega_j}{16\pi m_e \omega_i}f(\Delta E_{ji})A_a, \tag{18}$$

where ω_j and ω_i are statistical weights od double excited state and lower level and A_a is the autoionization (Auger) rate. The transition occurs at discrete energy ΔE_{ji} which corresponds to the energy difference between states. For the Maxwellian distribution, this equation leads to the well-known expression (Phillips at al., 2008)

$$C^{diel} = \frac{h^3}{2(2\pi m_e k_B T)^{3/2}} \frac{\omega_j}{\omega_i} e^{-\frac{\Delta E_{ji}}{k_B T}} A_a .$$ (19)

Similarly, for κ-distributions we can write

$$C_\kappa^{diel} = \frac{A_\kappa \, h^3}{2(2\pi m_e k_B T)^{3/2}} \frac{\omega_j}{\omega_i} \frac{A_a}{\left(1 + \frac{\Delta E_{ji}}{(\kappa - 1.5) k_B T}\right)^{\kappa+1}} ,$$ (20)

leading to the expression used in KAPPA package (Dzifčáková et al., 2015):

$$C_\kappa^{diel} = C_{Maxw}^{diel} \frac{A_\kappa e^{\frac{\Delta E_{ji}}{k_B T}}}{\left(1 + \frac{\Delta E_{ji}}{(\kappa - 1.5) k_B T}\right)^{\kappa+1}} .$$ (21)

6.2.4. Recombination and ionization from excited levels

Power-law dependence on energy for the cross-section of the radiative recombination σ_{RR} from the excited levels is assumed (Osterbrock, 1974)

$$\sigma_{RR} = \frac{C_{RR}}{E^{\eta+0.5}},$$ (22)

where C_{RR} is a constant and $\eta + 0.5$ is a power law index. Subsequently, for the radiative recombination rate of κ-distributions R_{RR}^κ it is possible to write (Dzifčáková et al., 2013)

$$R_{RR}^\kappa = R_{RR}^{Maxw} \frac{\Gamma(\kappa + \eta - 0.5)(1.5 - \eta)^\eta}{\Gamma(\kappa - 0.5)},$$ (23)

where R_{RR}^{Maxw} is Maxwellian radiative recombination rate.

The ionization rates from the excited levels are also included in CHIANTI 9. The approximations of κ-distributions by a sum of Maxwellians by Hahn and Savin (2012) were used

$$f_\kappa(E, T) = \sum_0^n a_n \times f_{Maxw}(E, c_n \times T),$$ (24)

where a_n and c_n are constants tabulated by Hahn and Savin (2012). The direct ionization rate of κ-distributed electrons from excited levels, $R_{DI}^\kappa(T)$, is

$$R_{DI}^\kappa(T) = \sum_0^{n_{max}} a_n \times R_{DI}^{Maxw}(c_n \times T),$$ (25)

where $R_{DI}^{Maxw}(T)$ is Maxellian averaged direct ionization rate.

These rates are included in the calculation of the excitation equilibrium by the same way as in CHIANTI 9.

CHIANTI 9 contains also joint ionization and recombination rates with included cascade effects for some ions. These rates cannot be separated from cascade effects and recalculated for κ-distributions, therefore, only Maxwellian rates are available for these ions.

6.2.5. Continuum

Besides of the calculations of the spectral line intensities, the KAPPA package also allows for calculation of non-Maxwellian continua (Dzifčáková et al., 2015). Dudík et al (2012) calculated continuum for the κ-distributions. They considered contributions from free-free and free-bound continuum only. The contribution from two-photon continuum can be neglected (Phillips et al. 2008).

Total emissivity of free-free continuum due to electron-ion bremsstrahlung for κ-distributions can be expressed (Dudík et al., 2012)

$$\epsilon_{ff}(\lambda, \kappa, T) = \frac{A_\kappa T^{1/2}}{\lambda^2} n_e n_H \sum_Z K_Z(\kappa, T) A_Z \int_0^\infty \frac{g_{ff}(y,w)}{\left(1+\frac{y+w}{\kappa-1.5}\right)^{\kappa+1}} dy, \quad [\text{erg cm}^{-3} \text{ s}^{-1} \text{ sr}^{-1} \text{ Å}^{-1}], \quad (26)$$

where A_Z is the element abundance relative to hydrogen, $w = hc/\lambda k_B T$ is scaled photon energy, g_{ff} is free-free Gaunt factor, and

$$K_Z(\kappa, T) = \frac{1}{4\pi} \frac{32\pi}{3} \frac{e^6}{m_e c^2} \sqrt{\frac{2\pi k_B}{3m_e}} \sum_k k^2 \frac{n_k}{n_Z}, \quad (27)$$

where k is the ionization degree. The bremsstrahlung spectrum is strongly enhanced for low values of kappa mainly at short wavelengths (Dudík et al., 2012, Figs. 2 and 3) in the comparison with the Maxwellian distributions.

The emissivity of free-bound continuum originated by recombination of κ-distributed electrons which forms k-times ionized ions of element X with excited electron on the level j can be expressed (Dudík et al., 2012)

$$\varepsilon_{fb}(\lambda, \kappa, T) = \frac{1}{4\pi} \sqrt{\frac{2}{\pi}} \frac{\varepsilon}{(m_e k_B T)^{3/2}} n_e n_H \sum_{k,X} \frac{n_{k+1}}{n_k} A_X \frac{\omega_j}{\omega_0} \sigma_j^{bf} A_\kappa \frac{1}{\left(1+\frac{\varepsilon - I_j}{(\kappa-1.5)k_B T}\right)^{\kappa+1}}, \quad (28)$$

where $\varepsilon = hc/\lambda = E + I_j$ is the photon energy, I_j is the ionization potential from the level j with statistical weight ω_j, and σ_j^{bf} is the ionization cross section from level j.

Free-bound spectra for the κ-distributions showed greatly enhanced ionization edges (Dudík et al., 2012, Fig. 5). This is mainly the result of the increase of low energy electrons for the κ-distributions comparing with the Maxwellian ones with the same temperature.

6.2.6. Effects and diagnostics

To demonstrate the effect of κ-distribution to a synthetic spectrum, in Figure 2 we depict synthetic spectrum calculated for the extreme non-thermal distribution, $\kappa = 2$ (red), and for the Maxwell distribution (black). For both spectra the constant electron density $N_e = 10^9$ cm^{-3} was adopted, and the line ratio of Fe XI 180.40 Å / Fe XII 195.12 Å was chosen to be equal. Thus it can be seen that κ-distribution enhances line intensities of some allowed lines and the diagnosed T is higher than for the Maxwell distribution.

The sets of synthetic spectra calculated under the assumption of κ-distribution allow for construction of diagnostic models. Picking up specific line ratios one can diagnose plasma parameters as κ, T, electron density and DEM under the assumption on non-thermal κ-distribution. The κ-distribution has significant influence on the diagnosed T. The diagnosed electron densities are typically lower than Mawellian ones, for $\kappa = 2$ by about 0.1 dex in the log.
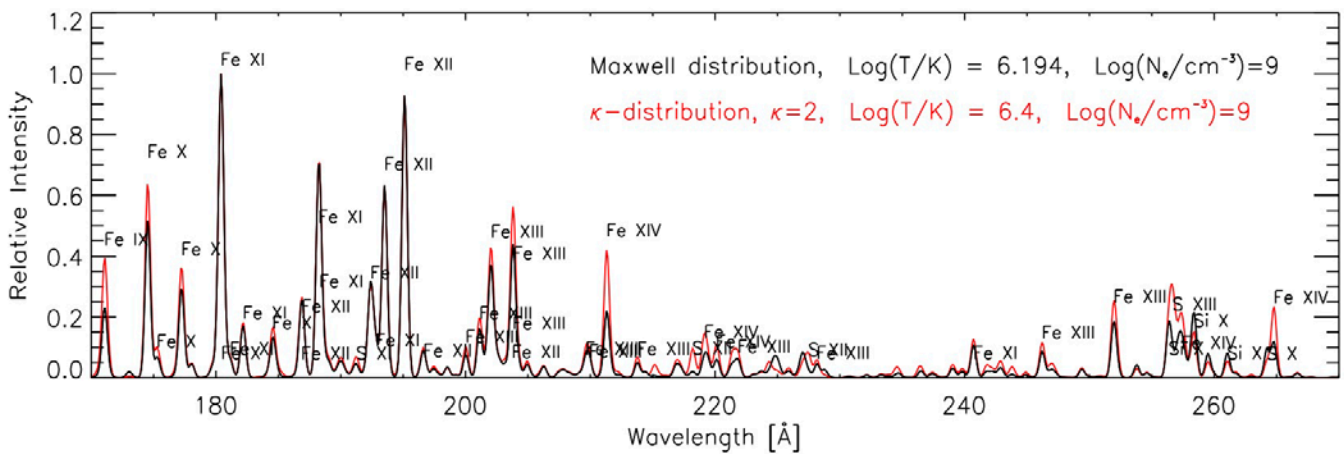
Figure 2. *Example of the synthetic spectrum calculated by KAPPA for the Maxwellian distribution (black line) and kappa-distribution with $\kappa = 2$ (red line). The line ratio of Fe XI 180.40 Å / Fe XII 195.12 Å is chosen to be the same in both spectra.*

Generally, a successful diagnostics of κ-distribution requires high precision of the observed line intensities. This requires good photon statistics as well as high precision of spectrometer calibration.

6.3. KAPPA package

The KAPPA database and software is based on CHIANTI, the freely available atomic database and software (Dere et al. 1997; Landi et al. 2013, Dere et al., 2019,). Similarly as CHIANTI, it works under Interactive Data Language (IDL). KAPPA software uses many modified CHIANTI routines and CHIANTI two ions model to calculate an excitation equilibrium.

The software and database of KAPPA package allows to calculate the synthetic spectra for integer values of $\kappa = 2, 3, 4, 5, 7, 10, 15, 25,$ and 33. These values of kappa allow for sufficient approximation to cover the observed cases. Ionization equilibria for these values of kappa are tabulated and included in database of the package.

The KAPPA package (kappa.asu.cas.cz) has its own, separate folders, where all routines and the database are located. It cannot be installed within the directory of CHIANTI itself in order to prevent its automatic removal by CHIANTI updates. The path to the folder can be set by an IDL system variable in the IDL `startup.pro` file:

`defsysv, '!data_pth', 'path to package'.`

The KAPPA folder contains original and the modified CHIANTI routines to calculate spectra for the κ-distributions, with the `data9_k` subfolder having the same structure as the CHIANTI's `dbase` subfolder.

In the past, the first versions of KAPPA package corresponding to CHIANTI 5.2 (Dzifčáková 2006b) contained directly the coefficients for the approximation of Ω. In this case, the calculation of the spectrum for the κ-distributions was approximately ten times longer compared with that of CHIANTI using the Maxwellian distribution. Therefore, following the second version (corresponding to CHIANTI 7, Dzifčáková et al., 2015), $\Upsilon_{ij}(T, \kappa)$'s were pre-calculated for a grid temperatures and κ and included into its database.

The KAPPA database contains ionization, recombination, excitation, and deexcitation rates for κ-distributions**.**

6.3.1. Database

Database of KAPPA package is located in 'data9_k' subfolder. It has the same structure as "dbase" subfolder in CHIANTI, e.g. for C we have directory `c/`. Each element has its own directory.

A series of ancillary data are contained in additional directories of 'data9_k' subfolder:

`'masterlist/'`	- the list of the ions currently present in the database (a copy from the CHIANTI database 9.0),
`'abundance/'`	- elemental abundance files (a copy from the CHIANTI database 9.0),
`'continuum/'`	- contains files for the continuum calculations (a copy from the CHIANTI database 9.0),
`'dem/'`	- DEM files (a copy from the CHIANTI database 9.0),
`'ioneq/'`	- ionization fraction files for kappa-distributions,
`'ip/'`	- ionization potentials (a copy from the CHIANTI database 9.0).

Element directories contain subdirectory for each ion. For example, in `'c/'` directory we have subdirectories e.g. for C I - C VII we have subdirectories `'c_1/'` - `'c_7/'`. The filename for each ion follows spectroscopic notation.

The subdirectories for ions within the database contain data for the ionization and recombination rates for the κ-distributions together with tabulated $\Upsilon_{ij}(T, \kappa)$ and $\Upsilon_{ji}(T, \kappa)$ files in the ASCII format and as well as IDL save files with the extension `'.sav'`. Files have their names according to the ion and the κ with extension `'.ups'` for $\Upsilon_{ij}(T, \kappa)$ and `'.dwns'` for $\Upsilon_{ji}(T, \kappa)$, e.g., `'fe_10_k2.ups'` for $\Upsilon_{ij}(T, \kappa)$ of Fe X and κ = 2. Current version of KAPPA package fully corresponds to the atomic data contained in the CHIANTI database version 9.0.

The ion atomic data taken from CHIANTI database 9.0 have a name corresponding to ion's name (e.g. 'c_4') and filename extension:

`'.elvlc'`	- Level labelling, energy (a copy from the CHIANTI database 9.0),

`'.wgfa'`   - wave lengths, Einstein probabilities for spontaneous emission,
                    oscillator strengths (a copy from the CHIANTI database 9.0),

`'.fblvl'`   - Data for the free-bound calculations (a copy from the CHIANTI
                    database 9.0),

`'.auto'`   - autoionization rates (a copy from the CHIANTI database 9.0)

Those depending on kappa have suffix '_k' plus value of kappa (e.g. `'c_6_k2'` means C VI data for the kappa-distribution with kappa=2). They have filename extensions

`'.ups'`   - scaled upsilons
`'.dwns'`   - downsilons
`'.sav'`   - upsilons + downsilons in IDL save file
`'.tionr'`   - total ionization rates
`'.trecr'`   - total recombination rates
`'.rrlvl'`   - level resolved radiative recombination rates
`'.cilvl'`   - level resolved ionization rates

6.3.2. Software

KAPPA can be run mainly on Macs and on PCs with Linux. KAPPA is not standalone and needs CHIANTI software and database. KAPPA directory contains all KAPPA routines. To preclude incompatibility problems with CHIANTI software due to its upgrade CHIANTI, the most important CHIANTI 9.3.1 routines are also located in the KAPPA directory and their names have suffix '_m' before the extension (e.g. `'ch_synthetic_m'`). Some of them have been also slightly modified.

All the IDL routines have documentation in their extensive headers giving detailed descriptions and examples.

The main widget-type routine `'kappa'` is based on the CHIANTI routine `'ch_ss'` and has the same widgets. It allows to select the type of calculation by the selection of the ionization equilibrium file. The ion-equilibrium file name (extension `'.ioneq'`) with `'kappa_'` plus the κ value (e.g. `'kappa_02.ioneq'`) selects calculation for the κ-distribution with $\kappa = 2$. The selection of the ion equilibrium file without this syntax runs Maxwellian calculations. Outputs from `'kappa'` can be in form of ASCII arrays or structures compatible with CHIANTI.

Some of main routines like `'ch_synthetic_k'`, `'izothermal_k'`, are modified CHIANTI routines having the same names but with an extra '_k' in their name. They can be called also directly from the command line. These routines follow the original CHIANTI routines as closely as possible. The calling parameters of these routines are kept the same, except that the first parameter is always the value of kappa. Their outputs are also arrays or structures compatible with CHIANTI. Corresponding main Maxwellian routines from CHIANTI are also located in KAPPA folder and their names have an extra suffix '_m' in their names. The routines usually have a list of options. We recommend to read them.

The other routines are typically original routines (e.g. for the free-free continuum). They can be called by the main routines or directly from the command line. As an input, they can require a structure produced as an output from other routines.

The output structures usually have the same tags as CHIANTI output but they have one extra tag with value of kappa. Therefore, they can be used as input to the original CHIANTI routines.

Please report to us any problems you might find using the software.

Table 1: List of main-level routines

Synthetic spectra	
kappa	Multi-purpose widget to calculate line intensities, synthetic spectra with the continuum, and various outputs.
ch_synthetic_k	Multi-purpose routine that calculates line intensities (without any abundance factor), output is an IDL structure.
isothermal_k	Computes spectra from isothermal plasmas, output is an IDL structure
make_kappa_spec_k	Creates a synthetic spectrum. Works with structures.
Line emissivities	
emiss_calc_k	Calculation of the emissivities of all lines of a specified ion over given ranges of temperature and density.
Continuum	
freefree_k	Calculation of the free-free (bremsstrahlung) continuum.
freebound_k	Calculation of the free-bound continuum.
Ionization and recombination	
read_rrlvl_k	Reads level resolved radiative recombination rates.
read_tion_k	Reads total ionisation rates.
read_trec_k	Reads total recombination rates.
Excitation rates	
excit_rate_kappa	Calculates excitation and de-excitation rates for the specified ion and transition over given range of temperature.
ups_kappa_interp	Converts KAPPA fits to upsilons (thermally-averaged collision strengths) for a specified κ-distribution, ion, transition and temperature

6.3.3. Routines

6.3.3.1. Line intensities calculation:

The routine 'ch_synthetic_k.pro' calculates line intensities assuming constant pressure or density (or a model T, N), without the abundance factor. The calling sequence is:

```
IDL> ch_synthetic_k, kappa, wmin, wmax, output=output, $
        err_msg=err_msg, msg=msg, $
        pressure=pressure, density=density, $
        model_file=model_file, all=all,sngl_ion=sngl_ion, $
        photons=photons, masterlist=masterlist, $
        save_file=save_file, verbose=verbose, $
        logt_isothermal=logt_isothermal, $
        logem_isothermal=logem_isothermal, $
        goft=goft, ioneq_name=ioneq_name, dem_name=dem_name, $
        noprot=noprot, rphot=rphot, radtemp=radtemp, progress=progress
```

where the most important inputs are

kappa	- κ value,
wmin, wmax	- minimum and maximum of wavelength range,
density	- the electron density,
ioneq_file	- the name of the ion-equilibrium file with full path. They must contain the same value of κ as has kappa in calling sequence, in other case software uses the default ion equilibrium file for the κ-distribution (e.g. 'kappa_02.ioneq' for κ=2),
logt_isothermal	- array of logarithmic temperatures

Detailed description of inputs, outputs and key words is in the header of the routine.

Example:

Calling sequence:

```
IDL> ch_synthetic_k, 2, 10., 20., output=str2, density=1.e+9,$
        ioneq_name=!data_path+'ioneq/kappa_02.ioneq',$
        logt_isothermal=6.8, /photons, /noprot, /all, $
        sngl_ion=['fe_17','fe_18']
```

calculates the line intensities in the spectral range 10 - 20 Å for κ = 2, log(T/K) = 6.8, density 10^9 cm^{-3}, without included proton rates, for two ions Fe XVII and Fe XVIII, and intensities are in photon cm^{-2} s^{-1} sr^{-1}. The output is a structure 'str2'. The structure is nearly the same as the output from CHIANTI 'ch_synthetic.pro', but it has a one more tag '.kappa' with the value of κ (see Appendix 2).

6.3.3.2. Continuum calculation

The routines 'freebound_k' and 'freefree_k' calculate intensities of the free-bound and free continuum for κ-distributions. The calling sequences are:

```
freebound_k, kappa, temp, wvl, int, sumt=sumt, photons=photons, $
            noverner=noverner, iz=iz, ion=ion, no_setup=no_setup, $
            min_abund=min_abund, dem_int=dem_int, verbose=verbose, $
            kev=kev, em_int=em_int
```

```
freefree_k, kappa, temp, wvl, int, min_abund=min_abund, $
            iabund=iabund, no_setup=no_setup, photons=photons, $
            ff=ff,int_precalc=int_precalc, $
            kev=kev, dem_int=dem_int, em_int=em_int, sumt=sumt
```

where the most important inputs are:

kappa	value of κ
temp	Temperature in K (can be an array).
wvl	Wavelength in angstroms (can be an array). If /keV is set, then WVL is assumed to contain energies in keV units.

Output is

int	free-bound continuum intensity, array [10^{-40} erg cm^3 s^{-1} sr^{-1} Å^{-1}].

Detailed description of inputs, outputs and key words is in the header of the routine.

Example:

Calling sequences:

```
IDL> freefree_k, 3, 5.e+6, findgen(50)+1.,ff
IDL> freebound_k, 3, 5.e+6, findgen(50)+1.,fb
```

calculate free-free and free-bound continuum for $\kappa = 3$, T = 5x10^6 K and for wavelengths at 1 Å intervals between 1 and 50 Å.

6.3.3.3. Calculation of synthetic spectra

Isothermal synthetic spectra for the κ-distributions can be calculated using routine **'isothermal_k'.** The calling sequence is:

```
isothermal_k, kappa, wmin, wmax, wavestep, temp, lmbda, spectrum, list_wvl, $
        list_ident, pressure=pressure, edensity=edensity, photons=photons, $
        ergs=ergs, sngl_ion=sngl_ion, abund_name=abund_name, ioneq_name=ioneq_name, $
        verbose=verbose, min_abund=min_abund, cont=cont, masterlist=masterlist, $
        noprot=noprot, radtemp=radtemp, rphot=rphot, em=em, all=all
```

where the most important inputs are:

kappa	value of κ
wmin	Minimum of the wavelength range in Å.
wmax	Minimum of the wavelength range in Å.
wavestep	Bin size of spectrum (in Å).
temp	Electron temperature (or array) in K.
edensity	Electron density in cm^{-3}.

Outputs are:

lmbda	Wavelength array of calculated synthetic spectrum
spectrum	Intensity array
list_wvl	A list of wavelengths for use with synthetic_plot.pro
list_ident	A list of line identifications for use with synthetic_plot.pro

Detailed description of inputs, outputs and key words is in the header of the routine.

The routine **'kappa'** is user-friendly, widget-based approach to calculate synthetic spectra. It is a modification of CHIANTI routine 'ch_ss'.

```
IDL > kappa
```

This widget allows the user to calculate synthetic spectra in two basic steps. Basically, you follow the various widgets from top left to lower right to set the desired parameters. First calculate the line intensities. These values can be saved for later use. Next, specify further parameters such as the elemental abundances and instrumental spectral resolution and then calculate and plot the spectrum. These values can also be saved for later use. The HELP buttons in the widget provide short descriptions of the required information. More details are given below.

SOLARNET Project Office
20

Leibniz-Institut für Sonnenphysik (KIS)
Schöneckstr. 6, 79104 Freiburg Germany
Tel.: +49-761-3198-224; Email: SOLARNET-office@leibniz-kis.de

SOLARNET

"This project has received funding from the European Union's Horizon 2020 research and innovation programme for the period January 2019 until December 2022 under Grant Agreement No 824135 (SOLARNET)"

Example:

Calling sequence:

```
IDL> isothermal_k, 5, 10., 20., 0.02, 8.e+6, lambda, spectrum, $
          list_w, list_i, edensity=3.e+9, sngl_ion=[fe_17, fe_18], /cont
```

calculates the isothermal spectrum of Fe XVII and Fe XVIII with continuum for the κ-distribution with $\kappa = 5$ in the spectral range 10 - 20 Å, bin size 0.02 Å, T = 8x10^6 K, and the electron density=10^9 cm^{-3}.

The routine **'make_kappa_spec_k'** creates synthetic spectra for the κ-distributions using an output from 'ch_synthetic_k':

```
make_kappa_spec_k, kappa, transitions, lambda, output, bin_size=bin_size, $
        instr_fwhm= instr_fwhm, wrange=wrange, all=all, $
        continuum=continuum, abund_name=abund_name, min_abund=min_abund, $
        photons=photons, file_effarea=file_effarea, $
        err_msg=err_msg, verbose=verbose, kev=kev, $
        no_thermal_width=no_thermal_width
```

where the most important inputs are:

kappa	value of κ
transitions	the structure created by ch_synthetic_k.pro.
lambda	array of wavelengths. If not defined as input, it is calculated on the basis of BIN_SIZE, and returned as an output.
bin_size	bin size in Angstroms of the spectrum.
wrange	allows a subset of the wavelength range to be turned into a spectrum.
instr_fwhm	instrumental FWHM (Angstroms).

Detailed description of inputs, outputs and key words can be found in the header of the routine.

Example:

Calling sequence:

```
IDL> make_kappa_spec_k, 2, str2, lambda, output, binsize=0.02, instr_fwhm=0.25, /all,
/continuum
```

calculates synthetic spectrum with continuum ('output', array) in the spectral range of input 'str2', with bin size 0.02 Å and instrumental FWHM 0.25 Å ('lambda', array).

6.3.3.4. Emissivity calculation

The function **'emiss_calc_k'** calculates emissivities of all lines of a specified ion over given ranges of temperature and density for the κ-distributions with specified κ. The calling sequence is:

```
emiss_calc_k, kappa, iz, ion, temp=temp, dens=dens, radtemp=radtemp, $
        rphot=rphot, path=path, no_de=no_de, noprot=noprot $
```

```
        quiet=quiet, pressure=presure, diel=diel, $
        ioneq_file=ioneq_file, abund_file=abund_file, $
        no_setup=no_setup, sum_mwl_coeffs=sum_mwl_coeffs, $
        radfunc=radfunc, no_calc=no_calc, noionrec=noionrec, $
        no_rrec=no_rrec
```

where the most important inputs are:

kappa	value of κ
iz	Either the atomic number of the ion, or the name of the ion in CHIANTI format (e.g., 'fe_17').
ion	The spectroscopic number of the ion (e.g., 12 = XII).
temp	Direct specification of the temperature range (log T). Default temperature corresponds to the maximum of the specific ion abundance
dens	Direct specification of the density range (log Ne). Default density range is 8 to 12 in .5 intervals

Detailed description of inputs, outputs and key words can be found in the header of the routine.

*Example***:**

Calling sequences:

```
IDL> output=emiss_calc_k(2,26, 12)
IDL> output=emiss_calc_k(2,'fe_12')
IDL> output=emiss_calc_k(2,26, 12, temp=[6.2], dens=findgen(5)+8.)
IDL> output=emiss_calc_k(2,'fe_12', temp=findgen(11)/100.+5.5, pressure=10.e+15)
```

calculate emissivity of Fe XII lines for κ-distribution with $\kappa = 2$. The first and the second output corresponds to default temperature and electron density, the third one corresponds to log(T/K) = 6.2 and default electron densities, and the fourth one to the temperature array from log(T/K)=5.5 to log(T/K) = 6.5 and pressure 10^{15} cm^{-3}. The output is a structure which is nearly the same as output from CHIANTI 'emiss_calc', but it has a one more tag '.kappa' with the κ value (see Appendix 2).

6.3.3.5. Calculation of electron excitation rates

The routine **'excit_rate_kappa'** calculates the excitation and de-excitation rates for κ-distributions for the specified ion and transition over given range of temperature.

```
excit_rate_kappa, kappa, ion, trans, temp, e_rate, d_rate
```

where

kappa	The value of κ.
ion	The name of the ion in CHIANTI format (e.g., 'fe_17').
trans	The index of transition, can be an array
temp	The temperature (in Kelvins), can be an array.
e_rate	The excitation rate associated with temperature.
d_rate	The de-excitation rate associated with temperature.

The routine calls `'ups_kappa_interp'` and `'read_kappa_ups'`

Example:
Calling sequence:

```
IDL> excit_rate_kappa, 2, 'fe_17', indgen(3), [8.e+6,9.e+6],e_rate,d_rate
```

calculates the excitation and de-excitation rates for the κ-distribution with κ=2, for transitions with index 0-2 (between levels 1 and 2, 3, 4) of Fe XVII for temperatures 8×10^6 K and 9×10^6 K. Resulting rates are in arrays with [3x2] elements.

6.4. Appendix 1 - Data

6.4.1 Upsilon and downsilon data files with the extensions **`'.ups'` or `'.dwns'`**

1-th line

Column	Format	ID	Comment
1	i7	n	number of transitions
2	i4	nt	number of temperatures

2-nd line
nt columns f5.2

3-rd - n+2 lines

Column	Format	ID	Comment
1	i3	ZET	element (ZET=26 - 'Fe')
2	i3	ION	ionization degree (ion=21 - XXI)
3	i4	L1	index of the lower energetic level
4	i4	L2	index of the lower energetic level
5	10.e3	DE	energy difference between levels L1 and L2 in Ry
6 - 6+nt-1	e12.5	UPS	Scaled upsilons

Comments are located at the end of data file between two '-1'.

The routine **`'read_kappa_ups'`** reads upsilons and downsilons for selected kappa-distribution:

```
IDL> read_kappa_ups, name, data_e, data_d, tmp, energy
```

Input:
name - name of the `'.ups'` or `'.dwns'` file with its full path and without its extension
        e.g. name=!data_path+'fe/fe_15/fe_15_k2'
Output:
data_e - double array(nt0,n) - scaled upsilons
data_d - double array(nt0,n) - downsilons
tmp - array(nt0) - temperatures (in Kelvin)
energy - array(n) - excitation energy

where
nt0 - number of temperatures, n - number of transitions

It is possible to restore `data_e`, `data_d`, `tmp`, and `energy` in the same format from IDL save file:

```
IDL> restore, name+'.sav'
```

The routine **'ups_kappa_interp'** reads and descales upsilons and downsilons for selected κ-distribution and required temperatures:

```
ups_kappa_interp, kappa, ion, te, ups_e, ups_d, energy
```

The routine calls: `read_kappa_ups`
Input:
kappa - κ value
ion - ion in CHIANTI format (e.g. 'fe_17')
`te` - temperature in K (can be an array) for which upsilons and downsilons are required
Output:
`data_e` - double array(nt,n) - upsilons
`data_d` - double array(nt,n) - downsilons
`energy` - array(n) - excitation energy

where
nt - number of te, n - number of transitions

6.4.2. Data for total ionization or recombination rate '.tionr', '.trecr'
1-th line

Column	Format	ID	Comment
1	i7	NT	number of temperatures

2-nd - NT+1 lines

Column	Format	ID	Comment
1	e12.4	TMP	temperatures (in Kelvin)
2	e12.4	TIONRATE	total ionization rates
or	e12.4	TRECRATE	total recombination rates

NT+2 line 1-st column   '-1'   i2 format   data end

Comments are located at the end of data file between two '-1'.

The routine **'read_kappa_tionr'** reads total ionization rates for selected κ-distribution:

```
IDL> read_kappa_tion, name, tmp, tionrate
```

Input:
name - name of the '.tionr' file with its full path and without its extension
     e.g. name=!data_path+'fe/fe_15/fe_15_k2'
Output:
tmp - array(nt) - temperatures
tionrate - array(nt) - total ionization rates
where
nt - number of temperatures

The routine **'read_kappa_trecr'** reads total recombination rates for selected κ-distribution:

```
IDL> read_kappa_trecr, name, tmp, trecrate
```

Input:
name - name of the '.trecr' file with its full path and without its extension
        e.g. name=!data_path+'fe/fe_15/fe_15_k2'
Output:
tmp - array(nt) - temperatures
trecrate - array(nt) - total ionization rates
where
nt - number of temperatures

The routine **'tionrec_rate_kappa'** calculates total ionization and rates for selected κ-distribution and temperature:

```
IDL> tionrec_rate_kappa, kappa, ion, te, tionr, trecr
```

The routine calls: read_kappa_tionr, read_kappa_trecr

Input:
kappa - κ value
ion - ion in CHIANTI format (e.g. 'fe_17')
te - temperature in K (can be an array) for which total ionization and recombination are required
Output:
tionr - array(n) - total ionization rates
trecr - array(n) - total recombination rates
where
n - number of te

6.4.3. Data for level resolved radiative recombination rate '.rrlvl'
1-th line

Column	Format	ID	Comment
1	i7	N	number of transitions
2	i7	NT	number of temperatures

2-nd line

	Format	ID	Comment
1 - NT column	e10.2	Temp	temperatures

3-rd - 2+N line

Column	Format	ID	Comment
1	i5	Z	atomic number
2	i5	ION	ion
3	i7	initial_level	initial level
4	i7	final_level	final level
5 - 4+N	e10.2	rate	rate

Comments are located at the end of data file between two '-1'.

The function **'read_rrlvl_k'** reads level resolved radiative recombination rates for the κ-distributions

```
IDL> str = read_rrlvl_k (kappa, fname, status)
```

Input:
kappa - κ value
fname - The name for an ion in CHIANTI format (e.g. 'fe_17')
Output:
Structure `str` with several tags: kappa, rates, temperatures, levels and references. The output structure is nearly the same as in CHIANTI but it has one more tag `.kappa` (see Appendix 2).

6.5. Appendix 2 - Output structures

ch_synthetic_k - output structure contains the line intensities and details of transitions in tags:
`.kappa`   float, κ value
`.lines`   a structure containing information about the lines with tags:
      `.iz`   integer, the atomic number of the elements (e.g., 26=Fe)
      `.ion`   integer, the ionisation stage (e.g., 17=XVIII)
      `.snote`   string, the identification of the ion (e.g., 'Fe XXIV d')
      `.ident`   string, the identification of the transition, configuration and terms in text form.
      `.ident_latex` string, the identification of the transition, configuration and terms in latex form.
      `.lvl1`   integer, the lower level of the transition
      `.lvl2`   integer, the upper level for transition.
      `.tmax`   float, the temperature of maximum emission of the line.
      `.wvl`   float, wavelength of the transition, in Angstroms.
      `.flag`   a flag -1 if the line has only theoretical energy levels or not. Otherwise 0.
      `.int`   float, the intensity of line (erg/cm^2/s/sr or phot/cm^2/s/sr)
      `.goft`   float, the G(T) of the line (optional /exclusive with .int).
`.ioneq_name`   string, the ion balance file used (full path).
`.ioneq_logt`   float array, the he Log10 T values associated.
`.ioneq_ref`   string, the references.
`.dem_name`   string, the differential emission measure file eventually used (full path).
`.dem`   float array, the Log10 DEM values
`.dem_logt`   float array, the Log10 T values associated.
`.dem_ref`   string, the DEM references.
`.model_name`   string indicating the model used.
`.model_file`   string, full path of the (Te,Ne) file if defined. Null string otherwise.
`.model_ne`   float (array), the Ne value(s).
`.model_pe`   float, the Pe value.
`.model_te`   float, the Te values if 'Function' is selected. Otherwise 0.
`.wvl_units`   string, the wavelength units.
`.wvl_limits`   float, the wavelength limits specified by the user.
`.int_units`   string, the intensity units.
`.logt_isothermal`   float (array), the Log10(T) values used.
`.logem_isothermal` float, the Log10(EM) values used.
`.date`   string, the date and time when the structure was created.
`.version`   string, the version number of the CHIANTI database used.
`.add_protons`   a flag (0/1) to indicate whether proton data were used
`.photoexcitation`   aA flag (0/1) to indicate if photoexcitation was included
`.radtemp`   float, the blackbody radiation temperature (if photoexcitation was included).
`.rphot`   float, distance from the centre of the star in stellar radius units (if photoexcitation was included).

emiss_calc_k - output structure contains the line emissivities and details of transitions in tags:

.kappa	integer, value of κ
.ion_name	string; contains ion name, e.g., 'Fe XII'
.lambda	float; contains wavelength
.level1	integer; contains lower level of transition
.lvl1_desc	string; gives configuration and term of lower level
.level2	integer; contains upper level of transition
.lvl2_desc	string; gives configuration and term of upper level
.flag	integer; a flag to mark particular transitions
.em	fltarr(nt,nd); contains emissivities at particular temperatures and densities.

read_rrlvl_k - output structure contains the level resolved radiative recombination rates and details of transitions in tags:

.kappa	integer, value of κ
.rate	float array, contains level resolved radiative recombination rates
.temp	float array; contains associated temperatures
.final_level	integer array; contains final levels of transition
.initial_level	integer array; contains initial levels of transition
.ref	string; references

References:

Del Zanna, G., Fernández-Menchero, L., Badnell, N. R.: 2015, Benchmarking atomic data for astrophysics: Si III, Astron. & Astrophys., 574, A99

Dere, K. P., Landi, E., Mason, H. E., Monsignori Fossi, B. C., Young, P. R.: 1997, *Astron. Astrophys. Suppl.*, 125, 149

Dere, K. P., Del Zanna, G., Young, P. R., Landi, E. and Sutherland, R. S.: 2019," CHIANTI - An Atomic Database for Emission Lines. XV. Version 9, Improvements for the X-Ray Satellite Lines", *Astron. Astrophys. Suppl.*, 241, 2, Id. 22.

Dudík, J., Dzifčáková, E., Karlický, M., Kulinová, A.: 2011, The bound-bound and free-free radiative losses for the nonthermal distributions in solar and stellar coronae, *Astron. & Astrophys.*, 529, A103,

Dudík, J., Del Zanna, G., Dzifčáková, E., Mason, H. E., Golub, L.: 2014, Solar Transition Region Lines Observed by the Interface Region Imaging Spectrograph: Diagnostics for the O IV and Si IV Lines, *Astrophys. J. Letters*, 780, L12

Dudík, J., Dzifčáková, E., Karlický, M., Kulinová, A.: 2011, "The bound-bound and free-free radiative losses for the non-thermal distributions in solar and stellar coronae", *Astron. Astrophys.,* 529, A103

Dudík, J., Kašparová, J., Dzifčáková, E., Karlický, M., Mackovjak, Š.: 2012," The non-Maxwellian continuum in the X-ray, UV, and radio range", *Astron. Astrophys.,* 539, A107.

Dzifčáková, E.: 2000, Electron Excitation Rates in the Solar Corona for non-Maxwellian Electron Distributions, *Solar phys.*, 196, 113

Dzifčáková, E.: 2006, The Inuence of the Electron κ-Distribution in the Solar Corona on the Fe VIII - Fe XV Line Intensities, *Solar Phys.* 234, 243

Dzifčáková, E., Kulinová, A.: 2003, Carbon and Oxygen Coronal Line Intensities for the Electron κ-Distribution, *Solar Phys.*, 218, 41

Dzifčáková, E., Mason, H.E.: 2008, Computation of non-Maxwellian Electron Excitation Rates for Ions of Astrophysical Interest: Fe XV - a Test Case, *Solar Phys.* 247, 301

Dzifčáková, E., Kulinová, A.: 2010, The Diagnostics of the Kappa-distributions from EUV Spectra, *Solar Phys.* 263, 25

Dzifčáková, E., Homola, M., Dudík, J.: 2011, The ionization equilibrium and are line spectra for the electron distribution with a power-law tail, *Astron. Astrophys.* 531, A111

Dzifčáková, E., Dudík, J.: 2013, H to Zn Ionization Equilibrium for the Non-Maxwellian Electron -distributions: Updated Calculations, *Astrophys. J. Suppl. Ser.* 206, 6

Dzifčáková, E., Dudík, J., Kotrc, P., Farnk, F., Zemanova, A.: 2015, KAPPA: A Package for Synthesis of Optically Thin Spectra for the Non-Maxwellian -distributions Based on the Chianti Database, *Astrophys. J. Suppl. Ser.* 217, 14

Dzifčáková, E., Vocks, C., Dudík, J.: 2017, Synthetic IRIS spectra of the solar transition region: Effect of high-energy tails, *Astron. Astrophys.,* 603, A14

Hahn, M., Savin, D.W.: 2015, A Simple Method for Modeling Collision Processes in Plasmas with a Kappa Energy Distribution, *Astrophys. J.* 809, 178

Kašparová, J., Karlický, M.: 2009, Kappa distribution and hard X-ray emission of solar flares, *Astron. Astrophys.* 497, L13

Landi, E., Young, P. R., Dere, K. P., Del Zanna, G., & Mason, H. E. 2013, CHIANTI—An Atomic Database for Emission Lines. XIII. Soft X-Ray Improvements and Other Changes, *Astrophys. J.*, 763, 86

Livadiotis, G., McComas, D.J.: 2013, Understanding Kappa Distributions: A Toolbox for Space Science and Astrophysics, *Space Sci. Rev.* 175, 183

Mackovjak, S., Dzifčáková, E., Dudík, J.: 2014, Differential emission measure analysis of active region cores and quiet Sun for the non-Maxwellian -distributions, *Astron. Astrophys.* 564, A130

Osterbrock, D. E. 1974, Astrophysics of gaseous nebulae

Phillips, K. J. H., Feldman, U., & Landi, E. 2008, Ultraviolet and X-ray Spectroscopy of the Solar Atmosphere (Cambridge University Press)

Scudder, J.D., Karimabadi, H.: 2013, Ubiquitous Non-thermals in Astrophysical Plasmas: Restating the Difficulty of Maintaining Maxwellians, *Astrophys. J.* 770, 26

Seely, J.F., Feldman, U., Doschek, G.A.: 1987, Observation of nonthermal energy distributions during the impulsive phase of solar ares, *Astrophys. J.* 319, 541